PRESTRESS LOSSES IN CAST-IN-PLACE POST-TENSIONED BRIDGES: ANALYSIS AND COMPARISONS WITH DESIGN CODES

Samer A. Youakim[1] and Vistasp Karbhari[2]
[1]Assistant Project Scientist, University of California, San Diego, CA
[2]Professor, University of California, San Diego, CA

ABSTRACT
Long-term prestress losses in concrete structures are caused by creep and shrinkage of concrete and relaxation of prestressing steel. Reasonably accurate prediction of these losses is important to ensure satisfactory performance of the concrete member under service loads. An analytical method is presented to predict the long-term prestress losses and the associated change in concrete stresses in cast-in-place post-tensioned bridges. It is assumed that prestress loading and bridge self weight are applied at the same time instant, and a single concrete type (same creep, shrinkage and modulus of elasticity properties) is used for the entire cross section.

It is shown that long-term prestress losses calculated using the current provisions of bridge codes can be underestimated or overestimated, depending on the concrete creep and shrinkage properties as well as the non-prestressed steel ratio. On the other hand, the remaining concrete compressive stresses after long-term losses have occurred are normally overestimated when using current codes; this could result in unexpected cracking under additional live loads.

Keywords: creep; long-term; prestress loss; relaxation; serviceability; shrinkage

INTRODUCTION
Creep and shrinkage of concrete and relaxation of prestressing steel cause long-term prestress losses in concrete structures. While it is generally accepted that long-term losses do not affect the ultimate capacity of a prestressed concrete member, reasonably accurate prediction of these losses is important to ensure satisfactory performance of concrete structures in service. If prestress losses are underestimated, the tensile strength of concrete can be exceeded under full service loads, causing cracking and unexpected excessive deflection. On the other hand, overestimating prestress losses can lead to excessive camber and uneconomic design.

The error in predicting the long-term prestress losses can be due to: (1) inaccuracy of the input parameters (creep and shrinkage of concrete and relaxation of prestressing steel); and (2) inaccuracy of the method of analysis used. The objective of this paper is to address the second source of inaccuracy by presenting a simple analytical method to estimate long-term prestress losses. The method satisfies the requirements of equilibrium and compatibility and avoids the use of empirical equations that cannot be accurate in all cases. The inaccuracy in the material

properties used can be mitigated by varying the input material parameters and establishing upper and lower bounds on prestress loss.

Several empirical equations are available in bridge codes[1-3] that give the long-term losses in prestressing tendons due to creep, shrinkage, and relaxation. These equations ignore, or consider empirically, the presence of non-prestressed steel; thus, equilibrium and compatibility are not satisfied. When these equations are used to give the prestress loss in the tendon, the common practice is to apply the calculated change in prestress force in reversed direction to the concrete section to obtain the long-term change in concrete stresses. An example will show that, in presence of non-prestressed steel, this practice overestimates the long-term compressive stresses, and as a result, unpredicted cracking can occur at critical extreme fibers under full service loads.

Sign convention

Axial force N is positive when it is tensile. Bending moment M and its associated curvature ψ are positive when they produce tension at the bottom fiber of the cross section. Stress σ and strain ε are positive for tension and elongation. It follows that shrinkage ε_{cs} is a negative quantity; also, the relaxation in prestressing steel $\Delta\sigma_{pr}$ and the loss in tension due to combined effects of creep, shrinkage, and relaxation $\Delta\sigma_{ps}$ is negative. The analysis is considered for a prestressed concrete section with its centroidal principal y-axis in vertical direction; the coordinate y of any concrete fiber or steel layer is measured downward from a reference point O (to be defined later).

PROPOSED EQUATION FOR PRESTRESS LOSS

The long-term prestress loss $\Delta\sigma_{ps}$ due to creep, shrinkage, and relaxation for a typical post-tensioned section (Fig. 1) is given by

$$\Delta\sigma_{ps} = E_{ps}\left\{ k_A(\Delta\varepsilon_{cc})_{free} + y_{ps}\left[k_I\Delta\psi_{free} + k_{cc}(\Delta\varepsilon_{cc})_{free}/h\right]\right\} + k_{ps}\,\Delta\overline{\sigma}_{pr} \tag{1}$$

where

$$k_A = \frac{A_c}{\overline{A}};\;\; k_I = \frac{I_c}{\overline{I}};\;\; k_{cc} = \frac{A_c y_{cc} h}{\overline{I}};\;\; k_{ps} = 1 - \frac{E_{ps}}{\overline{E}_c}\left(\frac{A_{ps}}{\overline{A}} + \frac{A_{ps}y_{ps}^2}{\overline{I}}\right) \tag{2}$$

$$(\Delta\varepsilon_{cc})_{free} = \varphi\,\varepsilon_{cc}(t_0) + \varepsilon_{cs};\;\; \Delta\psi_{free} = \varphi\;\psi(t_0) \tag{3}$$

$$\varepsilon_{cc}(t_0) = \varepsilon_1(t_0) + (y_{cc} - y_1)\,\psi(t_0) \tag{4}$$

The derivation of Eq. 1 is given elsewhere.[4] Equation 1 satisfies the equilibrium requirement as well as compatibility at non-prestressed steel layers and at the centroid of prestressing steel.

Definition of Symbols

The symbols used in Eqs. 1 through 4 are defined below:

Material parameters

E_{ns} and E_{ps} = moduli of elasticity of non-prestressed and prestressing steel, respectively

$E_c(t_0)$ = modulus of elasticity of concrete at time t_0

$\overline{E}_c = E_c(t_0)/(1+\chi\varphi)$ = age-adjusted elasticity modulus of concrete[5] to account for the creep effects of stresses applied gradually on concrete

φ, χ, and ε_{cs} = creep coefficient, aging coefficient, and shrinkage

$\Delta\overline{\sigma}_{pr}$ = reduced relaxation = $\chi_r\ \Delta\sigma_{pr}$, where χ_r is the reduced relaxation coefficient (0.7~ 0.8) and $\Delta\sigma_{pr}$ is the intrinsic relaxation.[6]

Geometry parameters

A_c = area of net concrete section, that is gross concrete section minus area of non-prestressed steel minus area of prestressing duct

A_{ns} and A_{ps} = areas of non-prestressed and prestressing steels, respectively

A_1 = area of the transformed section at t_0 composed of A_c plus $A_{ns}\left(E_{ns}/E_c(t_0)\right)$

$\overline{A}$ = area of age-adjusted transformed section composed of A_c plus $A_{ns}\left(E_{ns}/\overline{E}_c\right)$ plus $A_{ps}\left(E_{ps}/\overline{E}_c\right)$

I_c = second moment of A_c about its centroid

$\overline{I}$ = second moment of $\overline{A}$ about its centroid

y = coordinate of any point measured downward from O, centroid of $\overline{A}$

h = total thickness of section

Strain and stress

ε and σ = strain and stress in concrete, respectively

cc, 1, *free, ps* = subscripts referring, to centroid of A_c, centroid of A_1, the change in concrete strain if creep and shrinkage were unrestrained, and prestressing steel

$\psi = d\varepsilon/dy$ = curvature (slope of strain diagram)

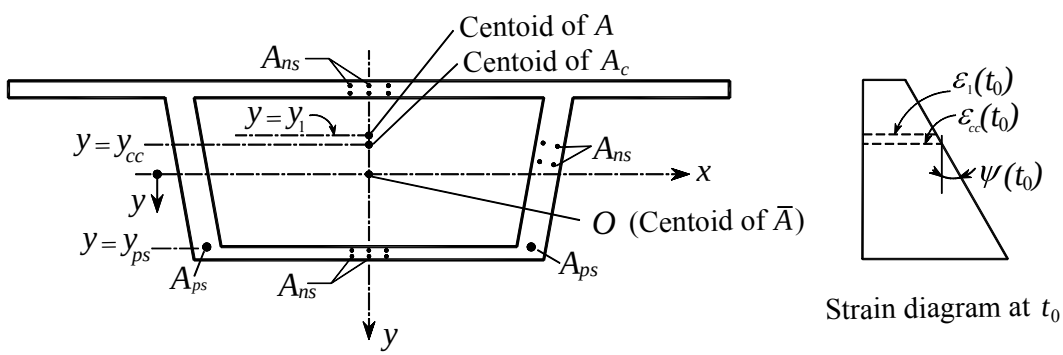

Fig. 1 Typical prestressed concrete section and strain diagram immediately after prestressing.

Long-Term Change in Concrete Stress

The time-dependent change in concrete stress at any fiber at distance y from O is

$$\Delta\sigma = \overline{E}_c\left(\Delta\varepsilon_O - (\Delta\varepsilon)_{free} + y\left(\Delta\psi - (\Delta\psi)_{free}\right)\right) \tag{5}$$

where $\Delta\varepsilon_O$ and $\Delta\psi$ are, respectively, the long-term change in strain at O and curvature:

$$\Delta\varepsilon_O = k_A(\Delta\varepsilon_{cc})_{free} - \frac{A_{ps}}{\overline{A}}\frac{\Delta\overline{\sigma}_{pr}}{\overline{E}_c} \tag{6}$$

$$\Delta\psi = k_I\,\Delta\psi_{free} + \frac{k_{cc}}{h}\left(\Delta\varepsilon_{cc}\right)_{free} - \frac{A_{ps}y_{ps}}{\bar{I}}\frac{\Delta\bar{\sigma}_{pr}}{\bar{E}_c} \tag{7}$$

PROVISIONS OF BRIDGE CODES

AASHTO-LRFD Refined Method[1]

The refined and approximate methods of AASHTO-LRFD are adopted by PCI-BDM.[7] The total long-term prestress loss $\Delta\sigma_{ps}$ is expressed as the sum of prestress loss due to creep, $\Delta\sigma_{ps(cr)}$; due to shrinkage, $\Delta\sigma_{ps(sh)}$; and due to relaxation, $\Delta\sigma_{ps(relax)}$ (kip-in. units):

$$\Delta\sigma_{ps(cr)} = 12\,f_{cgp} - 7\Delta f_{cdp} \tag{8}$$

$$\Delta\sigma_{ps(sh)} = -(13.5 - 0.123RH) \tag{9}$$

$$\Delta\sigma_{ps(relax)} = 0.3\left[-20 - 0.3\Delta\sigma_{ps(fr)} - 0.4\Delta\sigma_{ps(es)} - 0.2\left(\Delta\sigma_{ps(sh)} + \Delta\sigma_{ps(cr)}\right)\right] \tag{10}$$

where

f_{cgp} = concrete stress at center of gravity of prestressing steel at transfer

Δf_{cdp} = change in concrete stress at center of gravity of prestressing steel due to permanent loads applied after transfer

RH = relative humidity in percent

$\Delta\sigma_{ps(fr)}$ and $\Delta\sigma_{ps(es)}$ = prestress losses due to friction and elastic shortening, respectively.

AASHTO-LRFD Approximate Method[1]

For post-tensioned box-girder bridges with spans up to 160 ft (50 m), stressed at concrete age of 10 to 30 days with low-relaxation strands and subjected to average exposure conditions, the following approximate equations are suggested:

$$\Delta\sigma_{ps} = -(17 + 4PPR) \text{ (Upper bound)} \tag{11}$$

$$\Delta\sigma_{ps} = -(15 + 4PPR) \text{ (Average)} \tag{12}$$

PPR is the partial prestress ratio and is given by:

$$PPR = \frac{A_{ps}f_{py}}{A_{ps}f_{py} + A_{ns}f_y} \tag{13}$$

where

f_{py} and f_y = yield strength of prestressing and non-prestressed steel, respectively.

CEB-FIP Model Code[2]

The code gives the following equation for prestress loss due to creep, shrinkage, and relaxation:

$$\Delta\sigma_{ps} = \frac{\alpha_{ps}\varphi(t,t_0)f_{cgp} + E_{ps}\varepsilon_{cs} + 0.8\Delta\sigma_{pr}}{1 + \alpha_{ps}\dfrac{A_{ps}}{A_c}\left(1 + \dfrac{A_c y_{ps}^2}{I_c}\right)\left(1 + \chi\varphi(t,t_0)\right)} \tag{14}$$

where

$\alpha_{ps} = E_{ps}/E_c(t_0)$ = ratio of modulus of elasticity of prestressing steel to that of concrete

y_{ps} = y-coordinate of prestressing steel measured from the centroid of the net concrete section.

In Eq. 14, χ_r is taken 0.8 and the section is assumed to have a single layer of prestressing steel, without non-prestressed steel. In such a section, the requirements of equilibrium and compatibility are satisfied and Eq. 14 gives the same result as Eq. 1.

Canadian Highway Bridge Design Code[3] (CHBDC)

For post-tensioned concrete bridges with low-relaxation strands and ratio of the area of non-prestressed steel in tension to area of prestressing steel less than unity, CHBDC recommends the following equations, where f_{pu} is the ultimate strength of prestressing tendons:

$$\Delta\sigma_{ps(cr)} = 1.6\left[1.37 - 0.77(0.01RH)^2\right]\alpha_{ps}\left(f_{cgp} - \Delta f_{cdp}\right) \tag{15}$$

$$\Delta\sigma_{ps(sh)} = -(13.6 - 0.12RH) \tag{16}$$

$$\Delta\sigma_{ps(relax)} = -\left(\frac{\sigma_{p0}}{f_{pu}} - 0.55\right)\left(0.34 - \frac{\Delta\sigma_{ps(cr)} + \Delta\sigma_{ps(sh)}}{1.25 f_{pu}}\right)\frac{f_{pu}}{3} \geq 0.002 f_{pu} \tag{17}$$

ILLUSTRATIVE EXAMPLE

The two-span continuous post-tensioned bridge shown in Fig. 2 is subjected to its self weight and a uniform prestressing force *P* (after immediate losses) = 6200 kips (28,000 kN). It is required to:

1. Use the proposed method to find the long-term prestress loss and the change in concrete strains and stresses at two sections: Section A, at 50 ft from end support, and Section B, at intermediate support.
2. Use the equations of the bridge codes reviewed in the preceding section to calculate $\Delta\sigma_{ps}$ in Sections A and B and the stresses after long time, $\sigma(t)_{\text{bot}}$ in Section A and $\sigma(t)_{\text{top}}$ in Section B.

The bridge is located in an area with average relative humidity *RH* = 60%. The bottom slab thickness increases gradually in the 15 ft adjacent to the intermediate support from 7 to 12 in. Low relaxation strands of area A_{ps} = 31 in.^{2} (duct area = 62 in.^{2}) and f_{py} = 243 ksi are used in post-tensioning. The profile of the tendon is composed of two parabolas with common tangent at Section D. Use the following material properties: $E_c(t_0)$ = 3600 ksi (25 GPa); E_{ns} = 29000 ksi (200 GPa); and E_{ps} = 27500 ksi (190 GPa). The volume to surface ratio ≈ 6 in. The following material parameters are used: $\varphi = 2.6$; $\varepsilon_{cs} = -380 \times 10^{-6}$; $\Delta\sigma_{pr} = -6.6$ ksi $\chi = 0.8$; and $\chi_r = 0.7$. The values of φ and ε_{cs} are averages taken from AASHTO-LRFD, CEB-FIP, and CHBDC.

The values of $(A_{ns})_{\text{top}}$ and $(A_{ns})_{\text{bot}}$ given in Fig. 2(a) are used in the analysis described below. To study the effect of non-prestressed steel on concrete stresses and strains, additional results are given with the non-prestressed steel ignored and with the non-prestressed steel increased by 50%. Elastic analysis of the bridge subjected to self weight combined with prestress loading gives the strain and stress diagrams in Fig. 3(a) for Sections A and B immediately after prestressing. Figure 3(a) also gives the strain $\varepsilon_{cc}(t_0)$ at the centroids of the net concrete areas. The coefficients k_A, k_I, k_{cc}, and k_{ps} (Eq. 2) are given in Table 1.

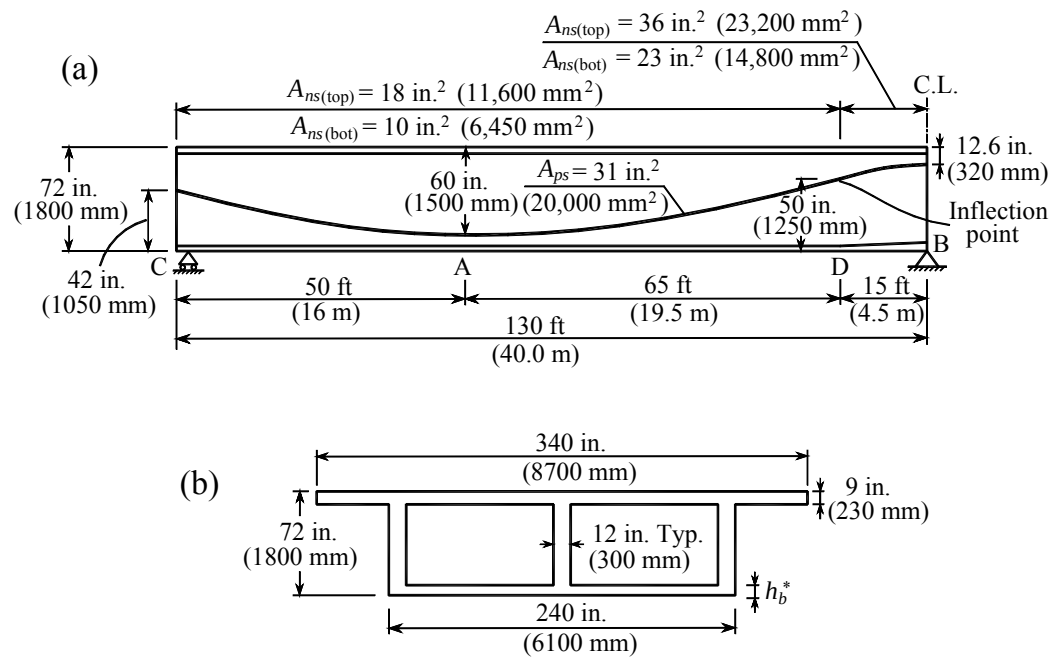

Fig. 2 Two-span continuous post-tensioned bridge. (a) Half elevation; (b) Cross section.

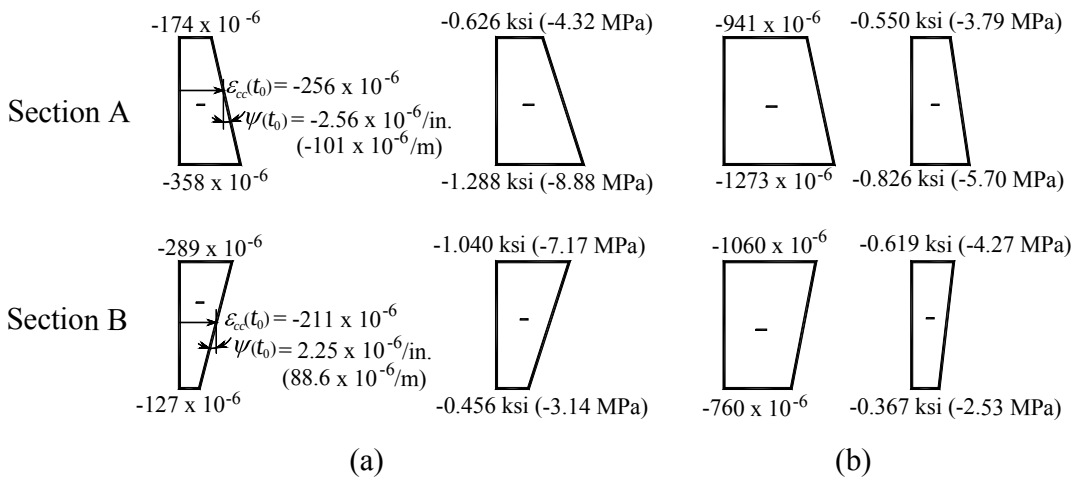

Fig. 3 Analysis of the bridge using proposed method. (a) Strains and stresses at time t_0; (b) Strains and stresses at time *t*.

The curvature, strains, and stresses at top and bottom fibers are listed in Table 2 for Sections A and B. Three sets of values are given corresponding to ignoring the non-prestressed steel, considering the non-prestressed steel as specified in Fig. 2(a), and considering that the non-prestressed steel areas are 1.5 times the areas in Fig. 2(a). The bottom fiber of Section A and the top fiber of Section B are the locations more vulnerable to cracking in service. Thus, prestressing is commonly designed such that sufficient compressive stresses remain after prestress loss. It can

be seen, by comparing the values printed in bold in Table 2, that ignoring the non-prestressed steel overestimates the absolute values of the compressive concrete stresses remaining at critical locations. The overestimation in the analyzed case is 0.156 and 0.353 ksi (1.08 and 2.43 MPa) at Sections A and B, respectively (column 4 minus column 8, Table 2); such overestimation can result in unexpected cracking and greater deflection than predicted due to live and other loads.

The concrete strains immediately after prestressing at the level of A_{ps} are -327×10^{-6} and -261×10^{-6} in Sections A and B, respectively (Fig. 3(a)). Multiplication by $E_c(t_0)$, gives f_{cgp} = −1.177 and −0.940 ksi (−8.12 and −6.48 MPa). In the AASHTO-LRFD approximate method, f_{py} and f_y are taken equal to 243 and 60 ksi, respectively and the sum of $(A_{ns})_{\text{top}}$ and $(A_{ns})_{\text{bot}}$ is used for A_{ns}. In Eq. 17 of CHBDC, the ultimate strength of the tendons f_{pu} is taken 270 ksi. It can be seen from Table 3 that the loss in tension in the prestressing steel, $\Delta\sigma_{ps}$, is either overestimated or underestimated by the codes. On the other hand, all the codes overestimate the concrete compressive stress remaining after long-term at the critical locations. The overestimation of the remaining compression increases with the increase of non-prestressed steel.

Table 1: Analysis for prestress loss using proposed method

Section	k_A	k_I	k_{cc}	k_{ps}	$\Delta\varepsilon_O$	$\Delta\psi$ (in.$^{-1}$)	y_{ps} (in.)	$\Delta\sigma_{ps}$ (ksi)
A	0.821	0.796	−0.197	0.823	-831×10^{-6}	-1.93×10^{-6}	27.5	−28.9
B	0.775	0.781	0.187	0.890	-707×10^{-6}	1.85×10^{-6}	−19.4	−25.1

Table 2: Concrete strains and stresses and curvature immediately after transfer and after long-term prestress loss (units: kip and in.)

Section		A_{ns} ignored		A_{ns} as given in Fig. 2(a)		A_{ns} increased by 50%	
		At transfer	Final	At transfer	Final	At transfer	Final
1	2	3	4	5	6	7	8
A	$\Delta\sigma_{ps}$	—	−31.6	—	−29.1	—	−28.0
	ψ	-2.63×10^{-6}	-4.48×10^{-6}	-2.56×10^{-6}	-4.61×10^{-6}	-2.52×10^{-6}	-4.63×10^{-6}
	ε_{top}	-179×10^{-6}	-1047×10^{-6}	-174×10^{-6}	-941×10^{-6}	-171×10^{-6}	-896×10^{-6}
	ε_{bot}	-368×10^{-6}	-1370×10^{-6}	-358×10^{-6}	-1273×10^{-6}	-353×10^{-6}	-1229×10^{-6}
	σ_{top}	−0.644	−0.671	−0.626	−0.550	−0.617	−0.499
	σ_{bot}	−1.325	**−0.934**	−1.288	**−0.826**	−1.271	**−0.778**
B	$\Delta\sigma_{ps}$	—	−30.3	—	−25.2	—	−23.2
	ψ	2.49×10^{-6}	6.03×10^{-6}	2.25×10^{-6}	4.16×10^{-6}	2.13×10^{-6}	3.29×10^{-6}
	ε_{top}	-309×10^{-6}	-1288×10^{-6}	-289×10^{-6}	-1060×10^{-6}	-280×10^{-6}	-971×10^{-6}
	ε_{bot}	-130×10^{-6}	-854×10^{-6}	-127×10^{-6}	-760×10^{-6}	-126×10^{-6}	-734×10^{-6}
	σ_{top}	−1.113	**−0.873**	−1.040	**−0.619**	−1.007	**−0.520**
	σ_{bot}	−0.468	−0.475	−0.456	−0.367	−0.453	−0.337

Table 3: Comparison of prestress loss and long-term concrete stresses calculated by codes' equations with values determined by the proposed method of analysis (units: ksi).

Section	Stress or stress change	Proposed method	AASHTO refined	AASHTO approximate	CEB-FIP Model Code	CHBDC
A	$\Delta\sigma_{ps}$	–29.1	–25.0	–18.3	–31.5	–25.9
	$(\sigma(t_0))_{\text{bot}}$	–1.288	–1.288	–1.288	–1.288	–1.288
	$\Delta\sigma_{\text{bot}}$	0.462	0.300	0.220	0.379	0.311
	$(\sigma(t))_{\text{bot}}$	–0.826	–0.988	–1.068	–0.909	–0.977
B	$\Delta\sigma_{ps}$	–25.1	–22.4	–17.8	–30.4	–22.8
	$(\sigma(t_0))_{\text{top}}$	–1.040	–1.040	–1.040	–1.040	–1.040
	$\Delta\sigma_{\text{top}}$	0.426	0.168	0.134	0.229	0.171
	$(\sigma(t))_{\text{top}}$	–0.619	–0.872	–0.906	–0.811	–0.869

DISCUSSION ON CODES

The empirical equations of the codes give accurate values of $\Delta\sigma_{ps}$ only in specific conditions. The equations of AASHTO-LRFD refined method and CHBDC contain relative humidity *RH* as independent variable in calculating the prestress loss due to creep and shrinkage. Although relative humidity is a major parameter, creep and shrinkage are also dependent upon the volume divided by the surface area and the concrete mix proportions (often represented by the specified compressive strength f'_c). Therefore, concrete shrinkage ε_{cs} and creep coefficients φ vary within a wide range. A typical box girder section with multiple cells is shown in Fig. 4. The effect of varying φ on the prestress loss due to creep for the bridge section is shown in Fig. 5. The section has the following geometric dimensions: $\Sigma b_w/b$ = 0.2; b_t/b = 1.5; h_t/h = h_b/h = 0.1; d_{ps} = 0.8h; and A_{ps} = (0.8/100)$h\Sigma b_w$.

The proposed method (Eq. 1) is used to calculate the prestress loss due to creep $\Delta\sigma_{ps(cr)}$ by setting ε_{cs} = 0, $\Delta\overline{\sigma}_{pr}$ = 0, and varying $\chi\varphi$. The ratios of non-prestressed steel in top and bottom slabs are assumed equal and $\Delta\sigma_{ps(cr)}$ is calculated for three ratios of ρ_{ns} = 0.2, 0.8 and 1.5%. At time t_0 immediately after prestressing, the concrete strains are assumed equal to zero and −460 × 10^{-6} at top and bottom fibers, respectively. The elasticity moduli used are: $E_c(t_0)$ = 3600 ksi; E_{ps} = 27,500 ksi; and E_{ns} = 29,000 ksi. As expected, Eq. 8 of AASHTO-LRFD gives constant $\Delta\sigma_{ps(cr)}$, independent of $\chi\varphi$. As shown in Fig. 5, the proposed method gives $\Delta\sigma_{ps(cr)}$ values that are almost linearly dependent upon $\chi\varphi$. Compared with the proposed method, the prestress loss according to AASHTO equation changes from overestimating to underestimating the creep losses as the creep coefficient increases.

SUMMARY AND CONCLUSIONS

Empirical equations for long-term prestress loss $\Delta\sigma_{ps}$ of several codes are reviewed. The codes do not give guidance on how to calculate the long-term changes in concrete stresses and strains.

Presumably, the ratio of the changes to the initial strain and stress due to prestress loading is the same as the ratio of $\Delta\sigma_{ps}$ to the initial tension. It is shown that this presumption is correct only in the absence of non-prestressed steel. The equation of the CEB-FIP Model Code gives the same $\Delta\sigma_{ps}$ as the proposed method for sections containing one layer of prestressing steel, without non-prestressed steel. The AASHTO-LRFD and CHBDC equations are functions of the relative humidity, *RH*, rather than the creep coefficient φ and the shrinkage ε_{cs}. For the same *RH*, the values of φ and ε_{cs} can vary with the concrete strength and the volume divided by the surface area. Thus the equations of the two codes cannot be accurate in all cases; it is shown that they overestimate $\Delta\sigma_{ps}$ in some cases and underestimate it in others.

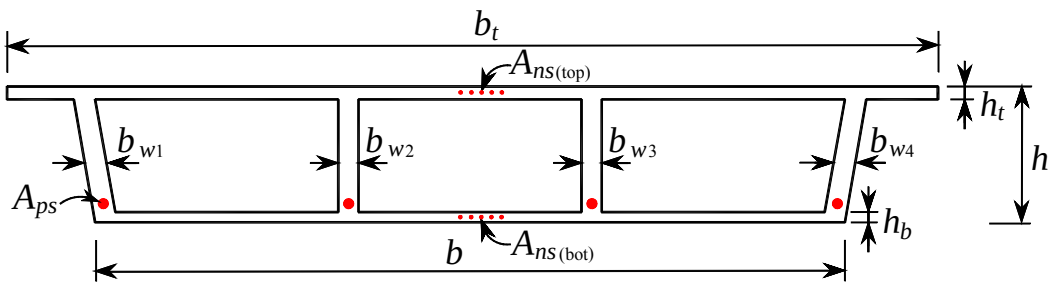

Fig. 4 Geometric dimensions and reinforcement in a typical bridge cross section.

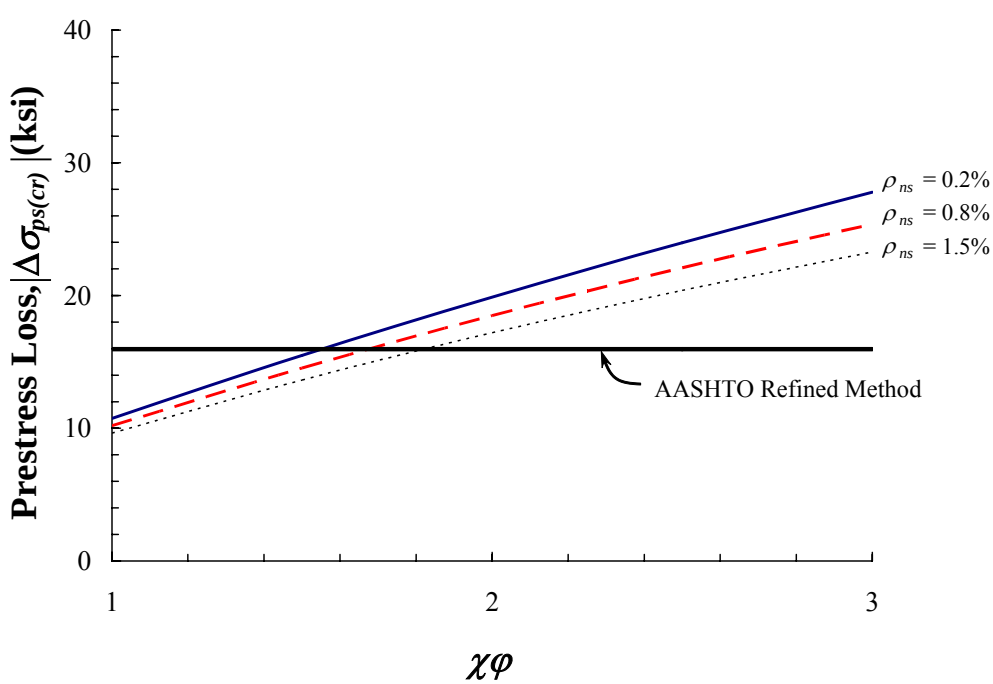

Fig. 5 Prestress loss due to creep: comparison between proposed method and AASHTO-LRFD refined method.

The proposed method of analysis is demonstrated by a worked example of a two-span bridge. The analysis is done with three different non-prestressed steel ratios. It is shown that at bottom fiber near mid-span and at top fiber over the interior support, the compressive stress remaining in concrete after losses has smaller absolute value as the amount of non-prestressed steel is increased. It is concluded that ignoring the non-prestressed steel, as is occasionally done in current design practice, can result in unexpected cracking and greater deflection than is predicted under subsequent live loads that occur in service.

REFERENCES

1. American Association of State Highway and Transportation Officials, "AASHTO-LRFD Bridge Design Specifications," Third Edition, Washington, DC, 2004.
2. Comité Euro-International du Beton − Fédération Internationale de la Précontrainte, "Model Code for Concrete Structures," CEB-FIP MC 90, London, UK, 1993.
3. Canadian Highway Bridge Design Code, CAN/CSA-S6-00, Rexdale, Canada, 2000.
4. Youakim, S.A., and Karbhari, V.M., "A Simplified Method for Prediction of Long-Term Prestress Loss in Post-Tensioned Concrete Bridges," *Caltrans Draft Report*, University of California at San Diego, CA, 2004, 64 pp.
5. Trost, H., "Auswirkungen des Superpositionsprinzips auf Kriech-und Relaxations-problems bei Beton und Spannbeton," *Beton und Stahlbetonbau,* V. 62, No. 10, 1967, pp. 230-238; No. 11, 1967, pp. 261-269 (in German).
6. Magura, D.D., Sozen, M.A., and Siess, C.P., "A Study of Stress Relaxation in Prestressing Reinforcements," *PCI Journal,* V. 9, No. 2, 1964, pp. 13-57.
7. Precast/Prestressed Concrete Institute, "Precast/Prestressed Concrete Bridge Design Manual," Sixth Edition, Chicago, IL, 2003.

ACKNOWLEDGEMENTS

The research reported in this paper was supported by California Department of Transportation under Research Grant No. 59A0420; this support is gratefully acknowledged.